Inference of Plausible Spatial Sizes of GRB Systems Using Newly Proposed FDSL-Model for GRB Time Delays

Godson Fortune Abbey[1], Joseph Simfukwe[1], Prospery Christopher Simpemba[1], Saul Paul Phiri[1], Alok Srivastava[1] and Golden Gadzirayi Nyambuya[1,2]

[1]Copperbelt University, School of Mathematics and Natural Sciences, Department of Physics, P. O. Box 21692, Jambo Drive Riverside, Kitwe, Republic of Zambia. E-mail: godsonabbey88@gmail.com, josephsimfukwe2013@gmail.com

[2]National University of Science & Technology, Faculty of Applied Sciences, Department of Applied Physics, P. O. Box AC 939, Ascot, Bulawayo, Republic of Zimbabwe. E-mail: physicist.ggn@gmail.com

We have used regression analysis to establish a time correction mechanism for four GRBs (030329, 980425, 000418, and 021004) employed from literature on the basis of a frequency-dependent speed of light (FDSL) model which we developed entirely from Maxwell's electromagnetic equations in conjunction with plasma and dispersion effects. In our first instalment (Paper 1), on the assumption that these GRBs all leave the source at the same time we obtained good positive correlations and hence justified the reliability of our fitting model. In this paper, however, on the assumption that each photon leaves the GRB source at different times, we modify the previous model to obtain a more fitting model. Furthermore, the modification led to the unification of the four GRBs into a homogenous albeit perfect correlation leading to the determination of the frequency equivalent of the ISM ($\nu_* = 1.507 \pm 0.0009\,\mathrm{Hz}$) and hence, the spatial sizes (ΔD) of the internal and external shocks wherein we obtain for the four GRBs $\Delta D = 838.90$, 39.00, 7804.00 and 19188.00 for GRBs 030329, 980425, 000418, and 021004 respectively. If the results provided herein are deemed acceptable or reasonable — *one can on this basis* — say that the relationship we have established from our analysis for the four GRBs supports two GRB models, "the framework of the fireball model" and "the multiple shock wave model" of GRBs production and their afterglow. Additionally, the implications are evident in the variations of relativistic outflows within the jets offering valuable insights into the acceleration mechanisms and interactions between the jet and its surrounding medium.

1 Introduction

One of the most puzzling phenomena in modern astrophysics is perhaps γ-ray bursts (GRBs). These brief flashes of non-thermal γ-ray energy which occur about once a day have consistently defied the *laws of physics* in their explanation. GRBs are highly concentrated high-energy explosions from distant objects deep within space. These explosions create a relativistic blastwave which inevitably collides with the circumburst medium resulting in internal and external shocks [1]. The photons emanating from these shocks possess enormous energies typically on the order of 10^{42}–10^{47} J [2, 3], and arrive at Earth as cosmic snipers that are uniformly distributed on the sky [4]. Due to these extreme energies, the prompt emission observed in these GRBs before now was believed to have been generated by a relativistic jet from their central engine [5–7]. Similarly, an afterglow is likely produced by external shocks from the interaction between the jet material and the circumburst medium [3].

Despite decades of research, the precise mechanisms driving GRBs and the characteristics of their progenitors remain a subject of intense investigation. One crucial aspect of understanding GRBs lies in estimating the spatial size of the shock waves they generate, as it provides invaluable insights into their physics and progenitor environments. Recent advancements in time-delay models, e.g. [8–11], have offered a promising avenue to infer the spatial scales of GRBs phenomena. These delays, resulting from the differential arrival times of photons emitted from different parts of the shock region encode valuable information about the size and structure of the emitting source. By exploiting the temporal behaviour of GRB emissions across different frequencies and utilizing theoretical models of light propagation and interaction with the surrounding medium, we can be able to constrain the spatial dimensions of GRB shockwaves.

However, such methods face limitations in resolving the intrinsic size of the shock region, often convoluted by the surrounding environment and instrumental effects. An alternative approach gaining traction involves exploiting the time delay phenomena observed in photons of different frequencies from GRB shocks as they propagate via the Interstellar Medium (ISM). This paper aims to provide an independent method formulated from relativistic mechanics in estimating the spatial size of GRB shocks using one of such time-delay models [8]. We will explore the theoretical foundations underpinning this model, the observational data utilized [12], and the constraints derived from such analyses. Additionally, we will discuss the implications of these spatial estimates on

our understanding of GRB physics, progenitor systems, and their broader astrophysical implications. In the end, we aim to provide insights into the spatial characteristics of GRB shocks and their implications for understanding the physics of these extraordinary cosmic events.

Penultimately, we shall give a synopsis of the remainder of the present article. To begin, in §2 we take a critical look at the GRB time delay shock models to understand the role these shocks play in the generation of photons of different frequencies as they travel through the ISM. §3 gives a brief overview of the fireball model with special emphasis on how the internal and external shock mechanism gives strong support for our ideas on the non-simultaneous release of the photon pairs. §4 discusses our proposed FSDL time delay model and how it all fits into our current instalment. In §5, we give a *step-by-step* process of the current time rectification methodology we adopted, the fitting procedure used to obtain ν_* and the constraints imposed on our parameters. §6, §7 and §8, present our results, the justification of our rectification mechanism and the general discussion accompanying our results. Thereafter, we conclude with §9.

Lastly, we perhaps must hasten and say that, throughout this paper, we assume a flat *Standard* ΛCDM-*Cosmology Model* where we take [13]: $\mathcal{H}_0 = 67.40 \pm 0.50\,\mathrm{km} \times \mathrm{s}^{-1} \times \mathrm{Mpc}^{-1}$, $\Omega_\Lambda = 0.685 \pm 0.007$, and $\Omega_m = 0.315$ and that, for all our calculations of the luminosity distances (D_L) to the different GRBs and their host galaxies, we shall use Wright's [14] online cosmology calculator.*

2 GRB Time Delay Models

Several studies provide valuable insights into the time delay mechanism of GRB shocks. e.g. [15] introduced an improved model-independent method based on time-delay measurements of GRBs at different energy bands. This method allows for probing the energy-dependent velocity due to modified dispersion relations for photons. Additionally, [16] discussed estimating the number of emitting electrons in GRBs based on fitted parameters and assuming specific emission radii predicted by shock models within the outflow. Moreover, [17] demonstrated how delayed and long-lasting afterglow emissions in certain GRBs could be interpreted through a synchrotron forward-shock model. This interpretation was supported by the analysis of radio, optical, and X-ray light curves. Many other authors have also studied time delay models in probing GRB to mention but a few [18]

This paper aims to provide an independent method formulated from relativistic mechanics in estimating the spatial size of GRB shocks using one of such time-delay models [8]. We will explore the theoretical foundations underpinning this model, the observational data utilized [12], and the constraints derived from such analyses. Additionally, we will discuss the implications of these spatial estimates on our understanding of GRB physics, progenitor systems, and their broader astrophysical implications. In the end, we aim to provide insights into the spatial characteristics of GRB shocks and their implications for understanding the physics of these extraordinary cosmic events. To begin, we will first take a critical look at the GRB fireball model with specific reference to the internal and external shock models to understand the role these shocks play in the generation of photons of different frequencies as they travel through the ISM.

3 Fireball Model

As is well known, a highly effective framework for interpreting observations of GRBs has been made available in the form of the fireball model [19–22]. The fireball model is commonly employed to explain the mechanism that produces the radiation we detect from most GRBs. The most widely accepted, and almost certain explanation for GRB production according to the fireball model is that when there is an ejection of extremely high energetic jets due to the merger of two neutron stars (NS-NS) [23], or a neutron star and a black hole (NS-BH) [4, 23] and a supernova [24] explosion as depicted in Fig. 1, the enormous release of energy gives rise to a Poynting-flux-dominated Magneto-hydrodynamics (MHD) wind with a luminosity of approximately $10^{50}\,\mathrm{erg} \times \mathrm{s}^{-1}$ [25] within the ISM confined to the jet cone. These MHD winds generate the GRBs when the kinetic energy of these ultra-relativistic particles, or potentially the electromagnetic energy of the Poynting flux, is converted to radiation [21, 26].

The GRB fireball model is essential for understanding the nature and implications of GRB shocks. In a bid to demystify the radiation mechanism, [27, 28] compared the fireball-shock and millisecond-magnetar models by fitting them to X-ray data of specific GRBs, emphasizing the importance of different shock models in explaining GRB phenomena. Similarly, [29] used a "boosted fireball" model to replicate the hydrodynamics of GRB outflows, highlighting the necessity for comprehensive models to decode the complexities of GRBs. In the same light, [30] provides a comprehensive review of γ-ray bursts and related transients, discussing theoretical models for prompt and afterglow emissions, including the standard fireball model with internal and external shocks. Their study highlights the role of synchrotron radiation from relativistic electrons accelerated in the shocks, emphasizing the importance of magnetic fields in these processes, and the internal and external shock mechanisms for γ-ray burst emission.

Additionally, [31] discussed utilizing GRB emissions as a test-bed for modified gravity theories, demonstrating how GRBs can offer insights into fundamental physics beyond standard models [32–35] and many more have also explored how gravitational wave observations can enhance our understanding of the intrinsic properties of the shock waves from GRBs, showcasing the interdisciplinary nature of studying

*https://www.astro.ucla.edu//~wright/CosmoCalc.html

these phenomena. To describe both the initial burst of γ-rays and the lengthy afterglow, the fireball model employs two separate shock wave models — namely, the *internal and external shock wave models* [36, 37].

3.1 Internal Shock

As depicted in Fig. 1, internal shocks are responsible for the high energy of γ-ray particles. Moments after the incident, shock waves (fronts) with a Lorentz factor (Γ) close to 100 are emitted from the inner engine at relativistic speeds leading to multiple shock waves, each travelling at a different relativistic speeds. These shock fronts result in energetic γ-ray emissions which are principally caused by thermal magnetic reconnection activities and relativistic processes. In this process, baryonic mass will be added to the emission, thus helping to convert some radiation energy into relativistic kinetic energy, which in turn increases the γ-ray burst flux. As illustrated in Fig. 1, a significant portion of the initial energy released by the freshly generated BH is transformed straight into photons in a pure radiation fireball [37, 38].

3.2 External Shock

On the other hand, external shocks are predominantly thermal emissions produced as the energy transferred from the shock waves is deposited into the interstellar medium (ISM). The spilt substance can then be trapped in the shock front and release radiation as the shock travels in the outward direction. The resulting broadband synchrotron radiation evolves as the external shock propagates outward into the surrounding medium, depending on various fundamental characteristics of the explosion, the specifics of the shock evolution, and the density profile of the medium into which it expands [26, 40]. When shocks from this external surrounding circumburst matter delay this flow of electrons, the afterglow appears with varying frequencies ranging from X-ray to optical wavelengths. It is generally assumed that most of the GRBs we detect are triggered by internal shocks, while the slow afterglow emanates from the external shocks [41].

It is on this theoretical explanation of this fireball model that we anchor our modified time delay emission model, wherein we now have the radio photon pairs not simultaneously leaving the GRB event as has been assumed in our previous papers [8]. We aim to show that under the above-stated new assumption of non-simultaneous emission of the radio photon pair, the time delay experienced by these photons may very well be a result of the series of shock waves generated by the internal and external production mechanism as is assumed in the fireball model. This may also lead us to understand the shock dynamics and/or the spatial sizes of the shocks.

4 Our Proposed FSDL Model

Here, we adopt a standard fireball scenario for the GRBs afterglow, where a relativistic shock with (Γ) expands into the circumburst medium (CBM). The afterglow flux arises from the radiation (synchrotron and possibly also inverse Compton) emitted by relativistic electrons accelerated from the internal to the external shocks. To describe the spatial size of these jets, we account for the effects of the conductance of the medium through which these radiations pass en route to the detector and model the shock dynamics using our FDSL-model.

The formulation we came up with was simple and elaborate which is: In [8], without any exogenous or exotic ideas being brought in, the following dispersion relation was derived directly from Maxwell's four fundamental equations of Electrodynamics

$$\omega^2 - {c_0}^2\kappa^2 = -4\omega_*\omega, \tag{1}$$

where $\omega_* = 2\pi\nu_* = \mu c^2\sigma/4, \omega = 2\pi\nu$, with ν being the frequency of the Photon and k its wave-number. Given that the group velocity ν_{g} of a wave is given by $v_{\mathrm{g}} = \partial\omega/\partial k$, thus differentiating Eq. (1) throughout with respect to k and rearranging, it follows that

$$v_g = \frac{c_0^2}{\omega/\kappa}\frac{1}{2\omega_*/\omega} = \frac{c_0^2}{v_p}\frac{1}{1+2\omega_*/\omega} = \frac{c_0^2}{v_p}\frac{1}{1+2v_*/v}, \tag{2}$$

where $v_p = \omega/k$, is the phase velocity. In a vacuum, we have that $v_g = v_p = c_0$. This assumption (of $v_g = v_p$) was extended to the scenario of a non-vacuum medium and so doing (i.e., maintaining this condition $v_g \neq v_p$, in the non-vacuum medium), one obtains

$$\frac{v_g}{c_0} = \frac{1}{\sqrt{1+\frac{2v_*}{v}}}. \tag{3}$$

From Eq. (3), it follows that if D is the distance between the Earth and the GRB, and v_l and v_h are the group velocities for the lower and higher frequency Photons, then - to first order approximation we have that $c_0/v_g \simeq 1 + v_*/v$, which in turns implies that for two photons with varying velocities, the time delay Δt is such that

$$\Delta t = \frac{D}{v_l} - \frac{D}{v_h} = \frac{Dv_*}{c}\left(\frac{1}{v_l} - \frac{1}{v_h}\right). \tag{4}$$

It is clear that if the laid down theory has any correspondence with physical and natural reality, then, a plot of $\Delta t \propto \left({v_l}^{-1} - {v_h}^{-1}\right)$ for the same source (i.e., same D) should accordingly yield a straight-line graph with a slope equal to Dv_*/c_0. Eq. (4) implies that the time delay will be given by

$$\Delta t = \frac{Dv_*}{C}\left(\frac{1}{v_l} - \frac{1}{v_h}\right). \tag{5}$$

The relation in Eq. (5) was applied to the following GRBs GRB 030329, GRB 980425, GRB 000418 and GRB 021004

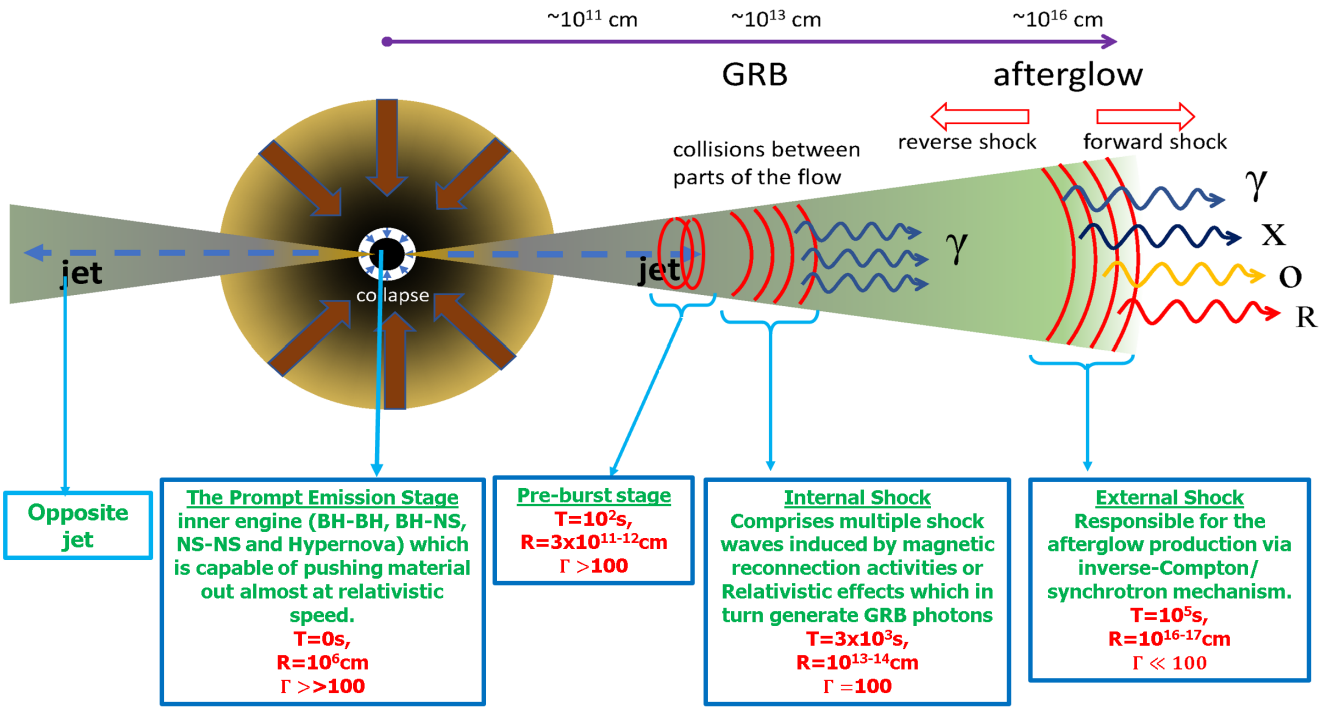

Fig. 1: A Modified cartoon depiction showing schematics description of and the basic mechanism of the GRB fireball model [39], https://www.swift.ac.uk/about/grb.php.

obtained from [12] and the result was a strong linear correlation between Δt and Δv^{-1}.

The obtained linear correlation confirms the theory on which Eq. (5) has been derived. Furthermore, in [8], as a major step, Eq. (5) assumes that the pair of GRB photons leave the event simultaneously. The above-stated assumption leads to a biased fit wherein the intercept of the graph of Δt vs $\Delta\nu^{-1}$ was made to pass through the point of origin $(0, 0)$ for there to be a zero y-intercept (see Fig. 2. Despite them giving a good correlation, the four graphs also yield slopes which were used to estimate the conductance of the ISM through which these GRB travel (see [8]).

In this current instalment, we develop a model that does not assume a simultaneous release of these pairs of photons. Rather preemptively, we must say that — this new assumption of a non-simultaneous — *albeit systematic* — emission of these photon pairs allows us to obtain a much more convincing and stronger correlation in the time delay. That is to say, this new correlation allows us to build a unified model of the four GRBs in our present sample wherein, we obtain two major results, mainly

1. A constant ν_* called the frequency equivalence of the interstellar medium (ISM)'s conductance which allows us to estimate every other parameter involved with the four GRBs in question;
2. The spatial sizes of the internal and external shocks of our four GRB samples.

One significant step involved in our modified FSDL model is the estimation of the time correction parameter t_c. In this modified model, we believe that a pair of events coming from the same shock front will lie on the same slope on a Δt vs $\Delta\nu^{-1}$ graph. In the case of our four GRB samples, the GRBs will be delayed by a fraction of the difference between the spatial sizes obtained from our calculation. Furthermore, in line with this assumption, the earlier photon leaves now while the latter leaves a time, t later. We can show that under the above-stated assumption, Eq. (5) will be modified to be

$$\Delta t = \frac{\mathcal{D}\nu_*}{c_0}\left(\frac{1}{\nu_l} - \frac{1}{\nu_h}\right) + t_c, \tag{6}$$

where t_c is a two-fold correction factor we introduced to rectify the time delay in the photon arrival times. Additionally, t_c is the y-intercept of this unbiased* linear regression model. This t_c will turn out to be the time difference between the emission of the photon pair from the internal and external shocks. This time difference is depicted in Figures 5 to 8 as the internal and external shock. We will briefly present our justification for our Non-simultaneous emission model.

4.1 Data Sampling and Description

As pointed out in Paper 1 [8], our data sample is wholly drawn from [12], wherein [12] draw their data from 304 GRB sam-

*By "unbiased plot", we mean a plot that does not force the linear graph to pass through the $(0, 0)$-point of origin as has been done on Paper 1.

ples compelled from 1997 to 2011 by [42]. From [12], eight of these GRB samples were used by [8] to investigate correlations in γ-ray burst time delays between pairs of radio photons as Paper 1 of a series of research geared towards investigating the cause of time delay in the arrival time of photons of different frequencies emanating from γ-ray burst.

In the said Paper 1 [8], in ascending order, the eight distinct GRBs we selected were 980425, 991208 000418, 000926, 021004, 030329, 031203 and 060218 making a total sample size of 52. Amongst these eight GRB samples, four of them GRB 980425, 000418, 021004 and 030329 when applied to our FDSL model gave good positive linear correlations as expected, which in turn provides a sound basis for our work and reliability of our model. The remaining four samples GRB 991208, 000926, 031203 and 060218 showed a weak correlation, so we didn't include them in our first instalment. In this present instalment, our aim was to put up a working model first with the 4 GRBs that gave a good positive correlation. To avoid constraints, we will differ the remaining weak correlated GRB samples to a later instalment where we can systematically test our model on all the data set in [12]. Additionally, we can now apply this model to recent data.

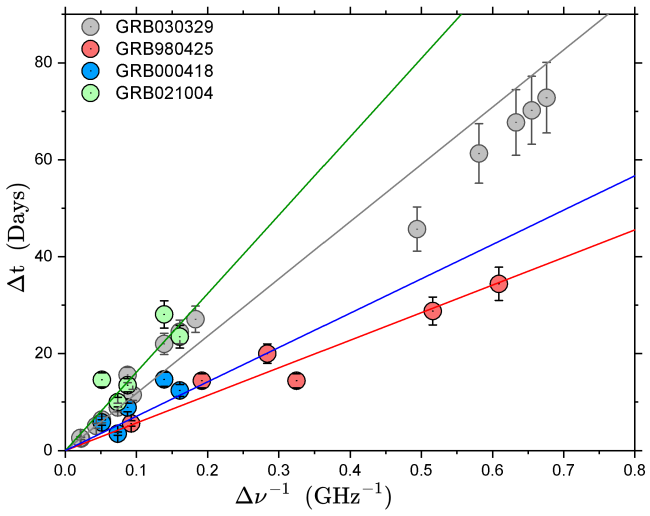

Fig. 2: Graph for Events GRB 030329, 980425, 000418, and 021004. The BLF were made to all passes through the origin.

5 Non-Simultaneous Photon Emission Model

Here we present a brief overview of our modified model as stated in the introductory section — the assumption that the low (ν_l) and high (ν_h) frequency photons are released simultaneously is to be done away with because it is very much possible that the low (or perhaps the high) frequency photon is released first, with the high (low) frequency photon is released a time t_c later (or *vice-versa*). In this event, the photon travel times t_l and t_h of the low and high frequency photons, respectively — will be related as follows

$$t_l = \frac{D}{v_l} + t_c, \tag{7a}$$

$$t_h = \frac{D}{v_h}, \tag{7b}$$

where, likewise v_l and v_h are the speed of the low and high-frequency photons, respectively. From the foregoing, it follows from Eq. (7), that

$$\Delta t = t_l - t_h = \frac{D}{v_l} - \frac{D}{v_h} + t_c. \tag{8}$$

As given in [8], if we are to substitute into Eq. (8), the following

$$\frac{1}{v_l} = \frac{1}{c_0}\left(1 + \frac{\nu_*}{\nu_l}\right), \tag{9a}$$

$$\frac{1}{v_h} = \frac{1}{c_0}\left(1 + \frac{\nu_*}{\nu_h}\right), \tag{9b}$$

then, one will be led to Eq. (5). In this way — as promised, we have justified Eq. (6).

It is important to note that if t_c is a random variable — *the meaning of which is that this time is not the same for each photon pair* — it would give rise to a clearly visible scatter in the data points along some imagined average straight line. If t_c is uniform for all the data points — imply some welcome define and systematic origin, then, the resulting data points — *if plotted in an unbiased manner* — they would lie on a straight line that does not pass through the $(0, 0)$-point of origin as is the case with the data point of the GRBs in our sample. In the next subsection, we will briefly describe how we obtained the ν_* from our t_c.

5.1 Fitting Procedures

As promised above, we here describe, in §5.1.1 & 5.1.1, the fitting procedures employed to arrive at a value for the time delay correction t_c and the value of the frequency equivalent of the ISM's conductance (ν_*).

5.1.1 Time Delay Correction (t_c)

To obtain t_c, the following procedures were carried out

1. First, we isolated the different subgroups of the individual GRBs as shown in Fig. 2. That is to say, we noted that for each GRB source, there exist two distinct subgroups — were for:
   (a) GRB 030329, as can be seen in Fig. 5, we have $(a, b, c, d, e, f, l, m, n, o)$ and (g, h, i, j) data points forming the two subgroups with GRB 0302329k being an outlier data point;

(b) GRB 980425, as can be seen in Fig. 6, we have (a, c, d) and (b, e, f) forming the two distinct subgroups;

(c) GRB 000418 of Fig. 7, have (a, d) and (b, c, e) forming the two distinct subgroups;

(d) Finally, GRB 021004, in Fig. 8 have (a, b, d) and (c, e) forming the two distinct subgroups;

2. Upon a meticulous observation of Fig. 5 to 8, one can see that the data points for the four GRBs were grouped in two; events group 1 representing the internal shocks and event group 2 representing the external shocks. The idea behind this grouping is to enable us to see the data points that are aligned so we can correct for the time delay (Fig. 7);
3. When the time delay (t_c) is corrected, one can see that each group's data points have been aligned into an almost straight line. Fig. 3 shows the same four GRBs in Figures 5 to 8 after t_c correction. The scattered and group events have been aligned almost perfectly to a straight line indicating a nearly perfect linear correlation amongst the four samples respectively.

5.1.2 Calculation of the Conductance (ν_*) of the ISM

At this point, we must say that, if our model is correct or has any meaningful correspondence with physical and natural reality, then ν_* can be obtained thus

1. First — we note that the slope of the time delay corrected graphs of Fig. 3 is proportional to the distances to the respective GRBs, i.e.

$$S = \frac{D\nu_*}{c_0}. \tag{10}$$

From this Eq. (10), it is clear that if the distance to the GRB is known, the value of ν_* can be computed. Further, if cosmological space is homogeneous, then ν_* must have a constant value in any given cosmological direction that one chooses. Assuming a homogeneous space as is the case in the ΛCDM-model [43], it follows that $S \propto D$, the meaning of which is that if the distance ($D_\dagger$) to just one GRB is known, then, the distance (D_k) to the rest of the GRBs can be inferred from this Eq. (10).

That is to say: let $S_\dagger$ be the slope on the graph of the GRB whose distance $D_\dagger$ is known and if S_k is the slope on the graph of the GRB whose distance D_k is unknown, then, we can deduce this distance D_k from the GRB whose slope $S_\dagger$ and distance $D_\dagger$ are known, i.e.,

$$D_k = \left(\frac{S_\dagger}{S_k}\right) D_\dagger. \tag{11}$$

From Eq. (10), it is abundantly clear that — *in-order to deduce* ν_* — one needs not know the actual distance to the GRB whose distance $D_\dagger$ is known, but a relative distance — e.g., $D_\dagger \equiv 1$, can be assigned, so that the relative distance $D_{\text{rel}}(k)$, to the k^{th} GRB on our list can be computed, i.e.,

$$D_{\text{rel}}(k) = \frac{S_\dagger}{S_k}. \tag{12}$$

From (11) and (12), it follows that

$$D_k = D_{\text{rel}}(k) D_\dagger. \tag{13}$$

It must be noted that $D_{\text{rel}}(k)$ is a dimensionless quantity while $D_\dagger$ has the dimensions of length;

2. Inserting D_k as given in Eq. (13) into Eq. (10), where Δt has been corrected for the non-simultaneous time delay, we will have

$$\frac{\Delta t}{D_{\text{rel}}} = \frac{D_\dagger \nu_*}{c_0}\left(\frac{1}{v_l} - \frac{1}{v_h}\right). \tag{14}$$

What Eq. (14) implies is that if all our assumptions are correct or have a meaningful correspondence with physical and natural reality, then, a plot of $\Delta t/D_{\text{rel}}$ *vs* $\Delta\nu^{-1}$ should yield a straight line graph. the result of the assumption is evident in (3);
3. In the present, for our standard GRB with distance $D_\dagger$ and slope $S_\dagger$, we took the GRB with the smallest redshift, namely GRB 980425, which has a redshift $z = 0.009$. The justification for doing this is spelt out in §7;
4. On careful observation of Fig. 4b one can see that the scatter in the plots has all been fully corrected into an almost perfectly straight line graph. A *t-test* was carried out on the combined plot to test for statistical significance. The result was not only consistent but also significant at a 95% confidence level. The complete regression fittings and other regression parameters are shown in Table 1 and 3;
5. Therefore, From the foregoing, we have that $D_\dagger = 40.00$ Mpc, and $S_\dagger = 70.00 \pm 2.00$ GHz × Days. Substituting these numerical values into 10 and converting to standard units we calculated v_* to be 1.507 ± 0.0009 as the frequency equivalence of the conductance of the ISM. Following we now estimate the spatial sizes of the internal and external shocks as presented in §6.

6 Result and Analysis

According to the Fireball model depicted in Fig. 1, a GRB will have two shock fronts, the internal and external. The events emanating from these shock fronts will have a large gradient on the Δt *vs* $\Delta\nu^{-1}$ graph. Given that in the present GRB time delay model, the distance (D) of the group events

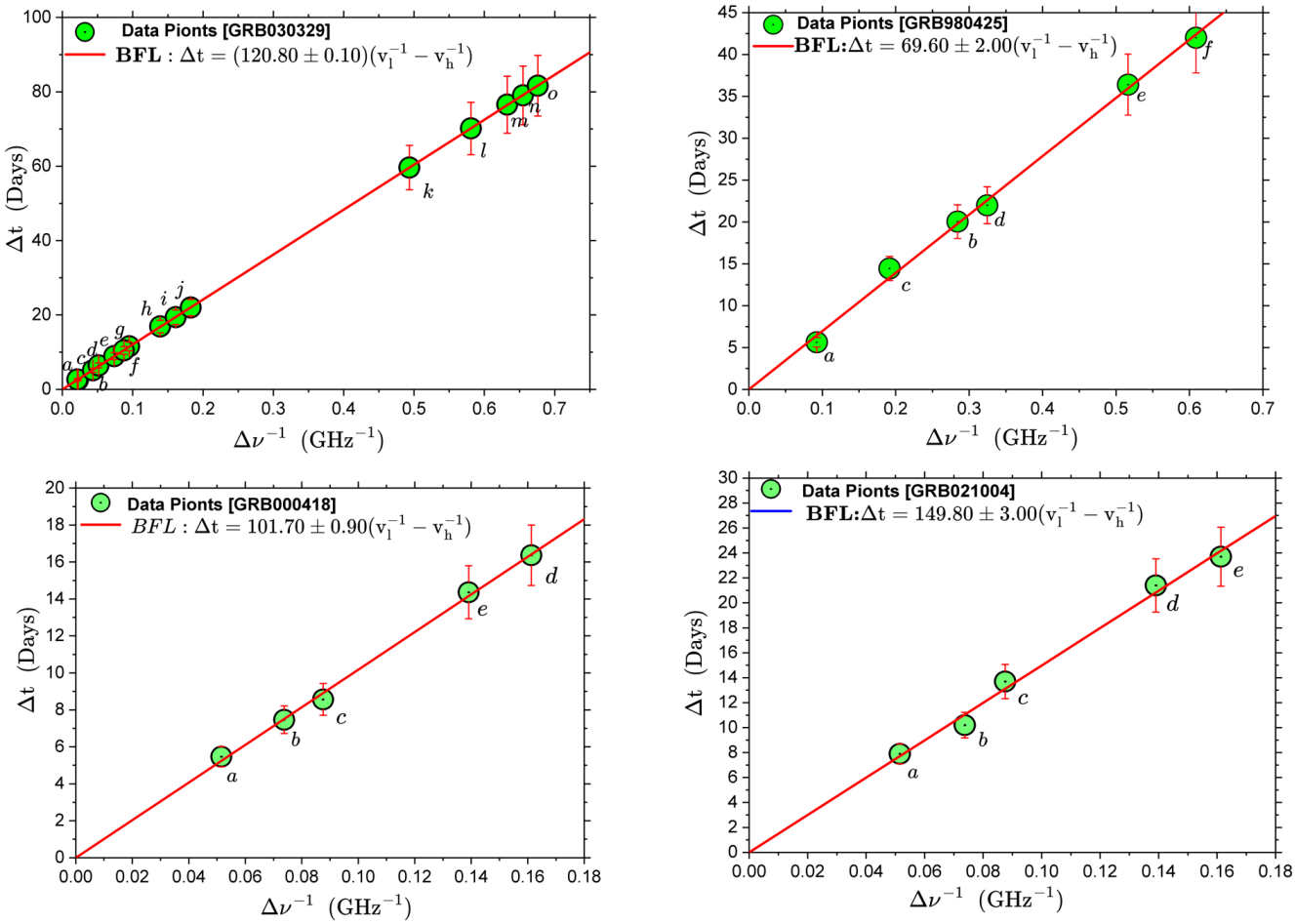

Fig. 3: Graph of GRB 030329, 980425, 000418, and 021004 events after t_C correction.

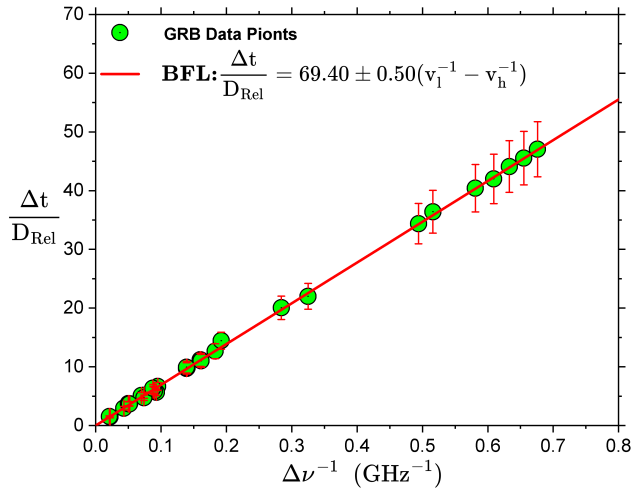

Fig. 4: Relative distance Plot. The combined scatter plots for GRB 030329, GRB 980425, GRB 000418 and GRB 021004 after relative distance correction respectively. Regression fitting for this plot passes through the $(0, 0)$-point of origin unbiased showing that the t_c has been eliminated naturally via our correction procedure

emanating from the same shock front is such that $D = c_0 S/\nu_*$. It follows from the foregoing that event group (1) must therefore be emanating from the internal shock while event group (2) are coming from the external shock. If both events have slopes S_1 and S_2, from the bare facts at hand, the spatial size, ΔD, between these two shocks is such that

$$\Delta D = \left(\frac{c_0 \Delta S}{v_*}\right) \tag{15}$$

where $\Delta S = S_2 - S_1$, $\Delta D = D_2 - D_1$ and $\nu_* = 1.507 \pm 0.009$ Hz (see [8]). Under the above premise, we now present the results of the spatial sizes of the four GRBs in question.

6.1 Estimating the Spatial Size

Following the procedures laid down so far, the spatial size (ΔD) can be estimated from the plot of Δt *vs* $\Delta\nu^{-1}$ as shown in Fig. 5 to 8 while keeping v_* as a constant. Fig. 5 to 8 shows a scattered plot of GRB 030329, GRB 980425, GRB 000418 and GRB 021004, with two fittings representing both the internal shocks (red line with yellow data points) and external shock (blue line with red data points). Regression analysis and fittings in accordance with the FDSL model yield the following result.

6.1.1 GRB 030329

GRB 030329 have a set of two events, namely — events $(a, b, c, d, e, f, l, m, n, o)$ and (g, h, i, j) as shown in Fig. 5, each with slopes $S_1 = 105.90 \pm 0.60$, and $S_2 = 120.80 \pm 2.00$ respectively. Substituting these values into Eq. 15 after converting to SI units with $\nu_* = 1.507 \pm 0.009$ Hz, we obtain the spatial size $\Delta D = 8.00 \pm 1.00$ Mpc. What this implies is that the spatial size between the jets is occurring at megaparsec scales. However, from the fireball model, this value seems to be very large compared to what has been obtained [49–51]. The significance is that the time delay is a result of the distance the Photons travel from the internal to the external shocks due to the reduction in their velocity as they travel via the ISM, thus making our fitting model more significant. It is also important to note that such distinct results greatly improve our understanding of GRBs if these results are to be corroborated with more data points.

6.1.2 GRB 980425

GRB 980425 have two events, namely — (a, c, d) and (b, e, f) forming the two distinct subgroups. as shown in Fig. 6, each with slopes $S_1 = 71.00 \pm 4.00$, and $S_2 = 75.00 \pm 8.00$ respectively. we obtain $\Delta D = 2.00 \pm 5.00$ Mpc. This GRB is also of the mega Parsec scale as expected.

6.1.3 GRB 000418

In the case of GRB 000418, we have two events, namely — events (a, d) and (b, c, e) as shown in Fig. 7, each with slopes $S_1 = 101.70 \pm 0.00$, and $S_2 = 102.40 \pm 7.00$ respectively. Substituting these parameters into 15, we obtain $\Delta D = 1.00 \pm 4.00$ Mpc. Similarly, the spatial size of this GRB is also of the mega Parsec scale as expected.

6.1.4 GRB 021004

Regression fittings for both the internal and external shocks for GRB 021004 are shown in Fig. 8. with $S_1 = 150.00 \pm 20.00$ and $S_2 = 154.00 \pm 0.00$ respectively, we obtain the spatial size to be $\Delta D = 13.00 \pm 4.00$ Mpc.

7 Interim Discussion

For the distances to the GRBs, we can use the ΛCDM-redshift distance estimates. Our reservation with this is that distances deduced using high redshift (i.e., $z > 0.009$) may not be accurate. For example, over the years, there has been a raging debate on this [52, 53]. This debate has somehow subsided with most astrophysicists and cosmologists accepting the ΛCDM-redshift distance estimates [54]. If any, there has not been any controversy with low redshifts and using these for distance determinations via Hubble's law [55, 56].

Rather fortuitously, we have in our four sample GRB the source GRB 980425 with a low redshift of $z = 0.0090$. This redshift is small enough so much that, one can easily apply the usual *Hubble law** to determine the distance to this

*On 26 October 2018, through an electronic vote conducted among all members of the International Astronomical Union (IAU), the resolution to recommend renaming the *Hubble law* as the *Hubble-Lemaître law* was accepted. This resolution was proposed in order to pay tribute to both —

Table 1: Result Table. In column 2 the number (1) is the internal shock and (2) is the external shock

Events	Shocks	Slopes for Shocks (S_1, S_2) (GHz × Days)	Slope ΔS $(S_2 - S_1)$ (GHz × Days)	y-Intercept (t_c) (t_{c1}, t_{c2}) (Days)	R^2
GRB 030329	(1)	105.90 ± 0.60	15.00 ± 2.00	+0.70 ± 0.20	0.9997
	(2)	120.80 ± 2.00		+5.00 ± 0.20	0.9997
GRB 980425	(1)	71.00 ± 4.00	4.00 ± 9.00	−9.00 ± 2.00	0.9975
	(2)	75.00 ± 8.00		−1.00 ± 2.00	0.9884
GRB 000418	(1)	102.00 ± 7.00	1.00 ± 7.00	−4.00 ± 0.00	1.0000
	(2)	102.00 ± 0.00		+0.30 ± 0.70	0.9949
GRB 021004	(1)	150.00 ± 20.00	10.00 ± 20.00	−0.30 ± 2.00	0.9889
	(2)	154.00 ± 0.00		+7.00 ± 0.00	1.0000

Table 2: Summary Table. Columns (1)-(4) lists (1) Source name, (2) Cosmological redshift of the host galaxies [44–48], (3) Distance to the GRB as obtained from Wright's cosmological calculator (4) the Spatial Size of the GRB shocks. The last row of the table presents the error-weighted average of the frequency equivalence of the conductance of the ISM, which we find to be $\nu_* = 1.507 \pm 0.009$ Hz.

Source	Host Galaxy Redshift	Distance ($\mathcal{D}_L$) (Mpc)	Spatial size (ΔD) (Mpc)
GRB 030329	0.1683 ± 0.0001	838.9000	8.0000 ± 1.0000
GRB 980425	0.0087 ± 0.0000	39.0000	2.0000 ± 5.0000
GRB 000418	1.1181 ± 0.0001	7804.0000	1.0000 ± 4.0000
GRB 021004	2.3304 ± 0.0005	19188.0000	13.0000 ± 3.0000

source without the need e.g. for Wright's [14] online cosmology calculator. If we can have confidence in the distance to this GRB as determined by Hubble's law, it means we can safely estimate the the ISM conductance σ. Taking $\mathcal{H}_0 = 67.4\,\mathrm{km} \times \mathrm{s}^{-1} \times \mathrm{Mpc}^{-1}$ [57], we obtain that the source GRB 980425 is at a distance of approximately, $\mathcal{D} = 40\,\mathrm{Mpc}$. Given that for this GRB, we have $\mathcal{D}\nu_*/c_0 = (6.00 \pm 2.00) \times 10^{15}$, it follows from all this — that, we will have that $\sigma = (1.0800 \pm 0.0400) \times 10^{-11}\,\Omega^{-1} \times \mathrm{m}^{-1}$. If what we have obtained is to be taken seriously, not only are these results consistent, but they also show a great possibility of querying the standard distance method adopted over the years for GRBs using redshift and cosmological methods.

8 General Discussion

The results we have obtained so far not only justify the authenticity of our model but also support the fireball model for the internal and external shock mechanism. Similar work has been done to understudy the mechanism of the internal and external shocks e.g. [33, 58–63]. One such major work by [64] delves into the width of γ-ray burst spectra as a measure to understand the emission processes in highly relativistic jets. Although the study highlights the differences in spectra widths, one can infer from this that such width may be a result of the large distances travelled by the photons indicating a large fraction across the jets. Similarly, [58] in a recent study investigated the long-term evolution of relativistic collisionless shocks in electron-positron plasma using $2D$ particle-in-cell simulations. Their results reveal the generation of intermittent magnetic structures by the shock, with magnetic coherence scales increasing over time as the photons travel along the jet cone. Their findings further suggest implications for γ-ray burst afterglow models, particularly in understanding the interplay between internal prompt emission and external shock mechanisms that power the afterglows in these astrophysical phenomena. Our findings and results also underscores the ongoing debate surrounding the

Georges Henri Joseph Édouard Lemaître (1894–1966), and, Edwin Powell Hubble (1889–1953), for their fundamental contributions to the development of the modern expanding cosmology model.

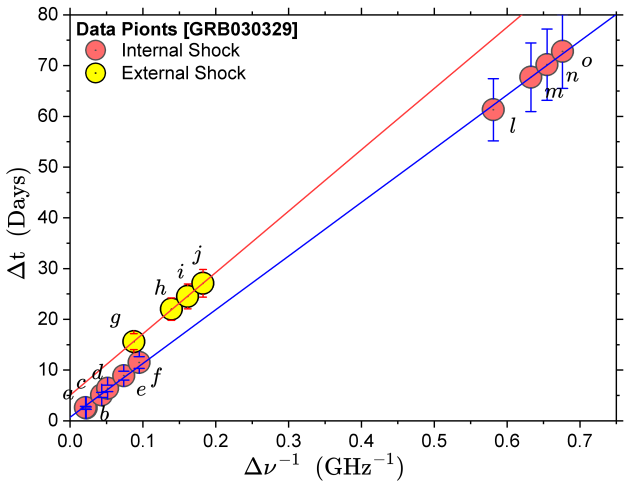

Fig. 5: Graph for Events GRB 030329 $(a, b, c, d, e, f, l, m, n, o)$ and (g, h, i, j). The BLF yields slopes of $S_1 = (105.90 \pm 0.60)\,x + (0.70 \pm 0.20)$ @ $R^2 = 9.9997$ and $S_2 = (120.80 \pm 2.00)\,x + (5.00 \pm 0.20)$ @ $R^2 = 0.9997$.

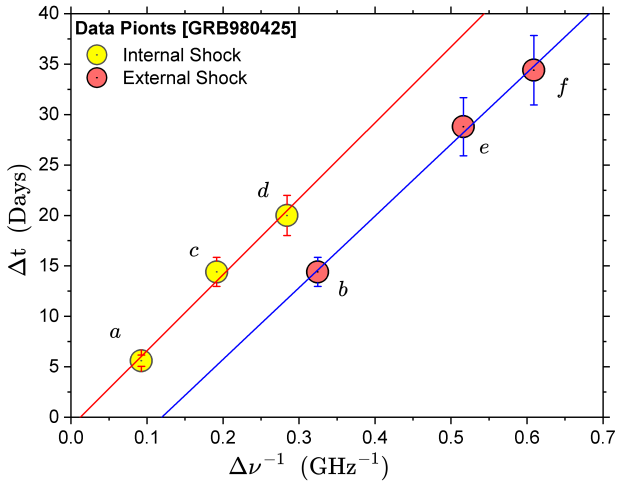

Fig. 6: Graph for Events GRB 980425 (a, c, d) and (b, e, f). The BLF yields slopes of $S_1 = (71.00 \pm 4.00)\,x + (9.00 \pm 2.00)$ @ $R^2 = 0.9975$ and $S_2 = (75.00 \pm 8.00)\,x + (1.00 \pm 2.00)$ @ $R^2 = 0.9884$.

internal and external shock mechanisms responsible for GRB emission which we believe is a step forward in the right direction.

For the internal shocks, one approach is to consider the variability timescale of the burst, which is related to the spatial size of the emitting region. On the other hand, the external shocks, are formed when the GRB outflow interacts with the surrounding medium, leading to a slower, and more prolonged emission phase.

This slowing down of the photons we believe is due to the vast difference between the internal and external shock which our model is accounting for. [65] has already shown that the radius of the external shocks can be estimated based on the deceleration timescale, which depends on the density of the surrounding medium. His findings agree with our rarefied plasma model as the interactions of the photons and the plasma medium through which these photons travel can significantly affect their propagation.

Additionally, as far back as the mid and late 1990's (see e.g. [21, 66]), it has been shown that the "*fireball model*" often used in GRB studies suggests that the internal shocks occur within the relativistic outflow produced during the GRB event. [67] further highlighted the transition from a stratified stellar wind to a homogeneous interstellar medium (ISM) and concluded that favourable parameters could lead to the detection of GRBs at hundreds of GeVs, emphasizing the importance of considering both internal and external shock mechanisms in understanding GRB emission dynamics. In both cases (internal and external shock mechanisms), detailed modelling and analysis of observational data, such as light curves and spectra, are necessary to constrain the parameters and obtain accurate estimates of the shock radii and possibly the spatial sizes.

This is the next phase of this work as we work to gather more data to carry out further analysis. What our model presents so far is in support of the fireball model but on a much larger scale. It is our hope that as we fine-tune this model and incorporate more data in subsequent work, we can be able to come close to what has been established and possibly improve on the existing knowledge of these extreme astrophysical phenomena.

It is paramount we bring this to the reader for better clarity that the spatial size of the internal and external shocks plays a significant role in determining how the photons and plasma interact and propagate through the ISM. Now, with regard to the interaction mechanism between the Photon and the plasma in the present model, one will rightly ask: *Since the Photon and the plasma are here interacting, what is different between this proposed interaction mechanism and the Plasma Effect*? To that, we have the following to say. The Compton wavelength of Photon — *or more so, its radius* — is much smaller than the wavelength of radio waves. From an intuitive physical standpoint, it is possible to imagine an Electron being engulfed by the Photon in such a manner that the Electron can be pictured to be moving inside the $\vec{E}$ and $\vec{B}$-fields of the Photon. Succinctly stated, the Electron is absorbed by the Photon in much the same manner as the Photon is absorbed by the Electron in such phenomenon as the *Photoelectric effect* [68], i.e., this simple but elaborate explanation will lead to our next instalment "can a photon absorb an electron".

It is our hope that our FSDL time delay model if properly fine-tuned with the right dataset will demystify the interaction mechanism between the photons and the plasma as they travel via the ISM.

Table 3: Combined Data Table [12]. Columns (1)-(8) list the (1) Initial/low frequency of the burst, (2) Final/high frequency of the burst (3) Initial time of the burst (4) Final time of the burst (5) Difference in the frequency (6) Values obtain from the two-fold correction (7) Relative distance obtained from the slopes of the four GRBs (8) Final values obtained from the relative distance correction

GRB Event Label	ν_1 (GHz)	ν_2 (GHz)	t_1 (Days)	t_2 (Days)	$\Delta\nu^{-1}$ (GHz^{-1})	Δt_c (Days)	D_{rel}	$\Delta t_c/D_{rel}$ (Days)
GRB030329a	15.00	22.50	8.40	10.90	0.022	2.56	1.7360 ± 0.0030	2.00 ± 0.10
GRB030329b	22.50	43.00	5.80	8.40	0.021	2.64	1.7360 ± 0.0030	2.00 ± 0.20
GRB030329c	15.00	43.00	5.80	10.90	0.043	5.14	1.7360 ± 0.0030	3.00 ± 0.30
GRB030329d	8.46	15.00	10.90	17.30	0.052	6.44	1.7360 ± 0.0030	4.00 ± 0.40
GRB030329e	8.46	22.50	8.40	17.30	0.074	8.94	1.7360 ± 0.0030	5.00 ± 0.50
GRB030329f	8.46	43.00	5.80	17.30	0.095	11.54	1.7360 ± 0.0030	7.00 ± 0.70
GRB030329g	4.86	8.46	17.30	32.90	0.088	10.49	1.7360 ± 0.0030	6.00 ± 0.60
GRB030329h	4.86	15.00	10.90	32.90	0.139	16.89	1.7360 ± 0.0030	10.00 ± 1.00
GRB030329i	4.86	22.50	8.40	32.90	0.161	19.39	1.7360 ± 0.0030	11.00 ± 1.00
GRB030329j	4.86	43.00	5.80	32.90	0.183	21.99	1.7360 ± 0.0030	13.00 ± 1.00
GRB030329k	1.43	4.86	32.90	78.60	0.494	59.65	1.7360 ± 0.0030	34.00 ± 3.00
GRB030329l	1.43	8.46	17.30	78.60	0.581	70.15	1.7360 ± 0.0030	40.00 ± 4.00
GRB030329m	1.43	15.00	10.90	78.60	0.633	76.55	1.7360 ± 0.0030	44.00 ± 4.00
GRB030329n	1.43	22.50	8.40	78.60	0.655	79.05	1.7360 ± 0.0030	46.00 ± 5.00
GRB030329o	1.43	43.00	5.80	78.60	0.676	81.65	1.7360 ± 0.0030	47.00 ± 5.00
GRB980425a	4.80	8.64	12.70	18.30	0.093	5.65	1.0000 ± 0.0000	6.00 ± 0.60
GRB980425c	2.50	4.80	18.30	32.70	0.192	14.45	1.0000 ± 0.0000	14.00 ± 1.00
GRB980425d	2.50	8.64	12.70	32.70	0.284	20.05	1.0000 ± 0.0000	20.00 ± 2.00
GRB980425b	1.38	2.50	32.70	47.10	0.325	21.60	1.0000 ± 0.0000	22.00 ± 2.00
GRB980425e	1.38	4.80	18.30	47.10	0.516	36.40	1.0000 ± 0.0000	36.00 ± 4.00
GRB980425f	1.38	8.64	12.70	47.10	0.609	42.00	1.0000 ± 0.0000	42.00 ± 4.00
GRB000418e	4.86	15.00	12.30	27.00	0.140	14.36	1.4600 ± 0.0100	10.00 ± 1.00
GRB000418b	8.46	15.00	12.30	18.10	0.050	5.46	1.4600 ± 0.0100	4.00 ± 0.40
GRB000418c	4.86	8.46	18.10	27.00	0.090	8.56	1.4600 ± 0.0100	6.00 ± 0.60
GRB000418d	4.86	22.50	14.60	27.00	0.160	16.37	1.4600 ± 0.0100	11.00 ± 1.00
GRB000418a	8.46	22.50	14.60	18.10	0.070	7.47	1.4600 ± 0.0100	5.00 ± 0.50
GRB021004a	8.46	22.50	8.70	18.70	0.074	10.2	2.1500 ± 0.0300	5.00 ± 0.50
GRB021004b	4.86	8.46	18.70	32.20	0.088	13.7	2.1500 ± 0.0300	6.00 ± 0.60
GRB021004d	4.86	22.50	8.70	32.20	0.161	23.7	2.1500 ± 0.0300	11.00 ± 1.00
GRB021004c	8.46	15.00	4.10	18.70	0.052	7.89	2.1500 ± 0.0300	4.00 ± 0.40
GRB021004e	4.86	15.00	4.10	32.20	0.139	21.39	2.1500 ± 0.0300	10.00 ± 1.00

9 Conclusion

We have used regression analysis to establish a time correction mechanism for four GRBs (030329. 980425, 000418, and 021004) employed from [12] on the basis of a frequency-dependent speed of light model (FDSL model) which we developed entirely from Maxwell's electromagnetic equations in conjunction with plasma and dispersion effects. In line with this model, on the assumption that these GRBs all leave the source at the same time, we have shown in our previous paper [8] that these four GRBs gave good positive correlations and hence reliable for testing our model. In this paper, however, on the assumption that each individual photon leaves the GRB source at different times, we modify the previous model to obtain a more fitting model. Additionally, the correction led to the unification of the four GRB into a homogenous albeit perfect correlation which led to the determination of the frequency equivalent of the ISM (v_*) and hence, the spatial sizes of the internal and external shocks.

If the results provided herein are deemed acceptable or reasonable — *one can on this basis* — make the following tentative conclusion regarding the implication of the spatial sizes of GRB internal and external shocks using our FSDL time delay model:

1. The relationship we have established from our analysis for the four GRBs, clearly supports two GRB models "the framework of the fireball model" and "the multiple shock wave model" of GRBs production and their afterglow.
2. From our regression analysis that here, we can infer that not only is our model reliable and consistent but was used to

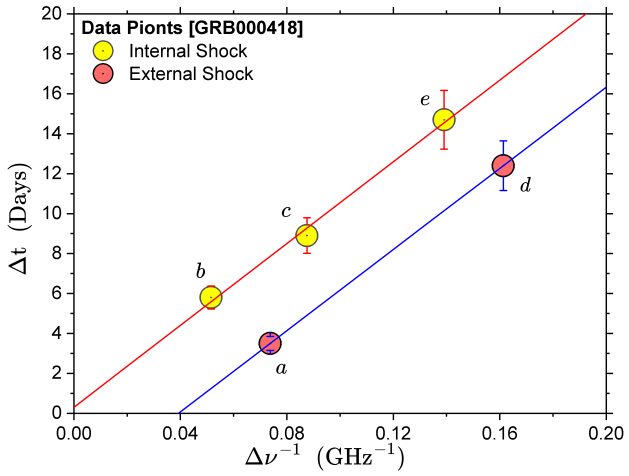

Fig. 7: Graph for Events GRB 000418 (b, c, e) and (a, d). The BLF yields slopes of $S_1 = (102.00 \pm 7.00)\,x + (4.00 \pm 0.00)$ @ $R^2 = 1.0000$ and $S_2 = (102.00 \pm 0.00)\,x - (0.30 \pm 0.70)$ @ $R^2 = 0.9949$.

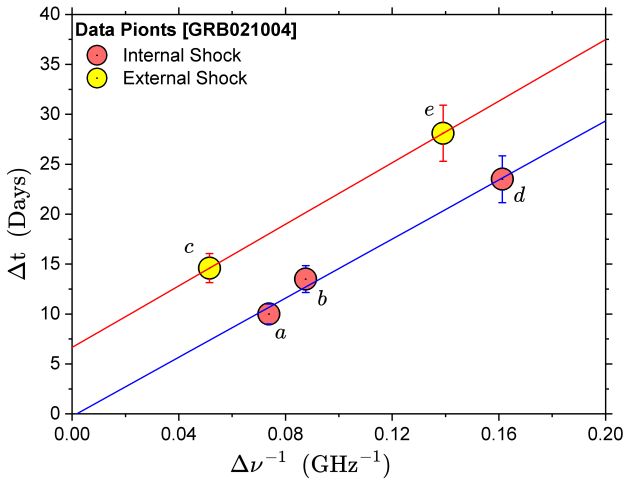

Fig. 8: Graph for Events GRB 021004 (b, c, e) and (a, d). The BLF yields slopes of $S_1 = (150.00 \pm 20.00)\,x + (0.30 \pm 2.00)$ @ $R^2 = 9.889$ and $S_2 = (154 \pm 0.00)\,x - (7.00 \pm 0.00)$ @ $R^2 = 1.0000$.

estimate the spatial sizes between the internal and external shocks.

3. From our FSDL time delay models and the fitting procedures we employ, we are able to say unequivocally that the internal shocks arise from variations in the relativistic outflows within the jet itself, which offer valuable insights into the acceleration mechanisms and particle interactions occurring within the jet. On the other hand, the external shocks, result from the interaction between the jet and its surrounding medium, which shed light on the environmental conditions and the impact of the jet on its surroundings. This we are able to deduce due to the nature of the differential time in the arrival time of the photons and the vast distances obtained in the spatial sizes between the internal and external shocks.

Furthermore, the determination of the spatial size of γ-ray jets for both internal and external shocks is a crucial endeavour in understanding the dynamics and emission processes of astrophysical jets. We believe that through meticulous observations, corroboration of more data sets and sophisticated modelling techniques for e.g. intense spectral analysis of the radiations from these shocks, 3D modelling of the particle dynamics emanating from the shocks, and magneto-hydrodynamic (MHD) effects, we can be able to unravel the complexities of these high-energetic phenomena.

Acknowledgements

We hereby acknowledge the financial support rendered by the Education, Audio and Culture Executive Agency of the European Commission through the Pan-African Planetary and Space Science Network under funding agreement number 6242.24-PANAF-12020-1-BW-PANAF-MOBAF. Also, we would like to acknowledge the invaluable support from our workstations — The Copperbelt University (Republic of Zambia) and the National University of Science and Technology (Republic of Zimbabwe) for the support rendered in making this work possible.

Submitted on June 17, 2024

References

1. Joshi J.C., Chand V., and Razzaque S. Synchrotron and synchrotron selfcompton emission components in GRBs detected at very high energies. *Proceedings of the 16th Marcel Grossmann Meeting*, 5–10 July 2021, World Scientific, 2023, 3009–3016.
2. Piro L., De Pasquale M., Soffitta P., et al. Probing the environment in gamma-ray bursts: the case of an x-ray precursor, afterglow late onset, and wind versus constant density profile in GRB 011121 and GRB 011211. *The Astrophysical Journal*, 2005, v.623, no.1, 314–324.
3. Ze-Cheng Zou, Bin-Bin Zhang, Yong-Feng Huang, and Xiao-Hong Zhao. Gamma-ray burst in a binary system. *The Astrophysical Journal*, 2021, v.921, id2, 1–7.
4. Janiuk A. Many faces of accretion in gamma ray bursts. arXiv: 2112.14086, 2021.
5. Bromberg O., Nakar E., and Piran T. Are low-luminosity gamma-ray bursts generated by relativistic jets? *The Astrophysical Journal Letters*, 2011, v.739, no.2, L55, 1–12.
6. Konigl A. Relativistic jets as X-ray and gamma-ray sources. *The Astrophysical Journal*, 1981, v.243, 700–709.
7. Kumar P., Zhang B. The physics of gamma-ray bursts & relativistic jets. *Physics Reports*, 2015, v.561, no.12, 1–109.
8. Nyambuya G.G., Marusenga S., Abbey G.F., Simpemba P., Simfukwe J. Correlation in gamma-ray burst time delays between pairs of radio photons. *International Journal of Astronomy and Astrophysics*, 2023, v.13, 195–216.
9. Hao J.M., Yuan Y.F. Progenitor delay-time distribution of short gamma-ray bursts: Constraints from observations. *Astronomy & Astrophysics*, 2013, v.558, A22.
10. Mao Shude. Gravitational lensing, time delay, and gamma-ray bursts. *The Astrophysical Journal*, 1992, v.389, no.2, L41–L44.

11. Zhang B., Zhang B. Gamma-ray burst prompt emission light curves and power density spectra in the ICMART model. *The Astrophysical Journal*, 2014, v.782, no.2, id92, 1–11.
12. Zhang B., Chai Y.T., Zou Y.C., Wu X.F. Constraining the mass of the photon with gamma-ray bursts. *Journal of High Energy Astrophysics*, 2016, v.11–12, 20–28.
13. Ade P.A., Aghanim N., Alves M.I., et al. Planck 2013 results. I. Overview of products and scientific results. *Astronomy & Astrophysics*, 2014, v.571, A1, 1–66.
14. Wright E.L. A cosmology calculator for the world wide web. *Publications of the Astronomical Society of the Pacific*, 2006 v.118, no.850, 1711–1715.
15. Pan Y., Qi J., Cao S., Liu T., Liu Y., Geng S., Lian Y., Zhu Z.H. Model-independent constraints on Lorentz invariance violation: implication from updated Gamma-ray burst observations. *The Astrophysical Journal*, 2020 v.890, no.2, id169, 1–7.
16. Burgess J.M., Bégué D., Greiner J., Giannios D., Bacelj A., Berlato F. Gamma-ray bursts as cool synchrotron sources. *Nature Astronomy*, 2020 v.4, no.2, 174–179.
17. Fraija N., De Colle F., Veres P., Dichiara S., Duran R.B., A.C. Caligula do E.S. Pedreira, Galvan-Gamez A., Kamenetskaia B.B. Description of atypical bursts seen slightly off-axis. *The Astrophysical Journal*, 2020, v.896, no.1, id25, 1–22.
18. Alexander K.D., Laskar T., Berger E., Johnson M.D., Williams P.K., Dichiara S., Fong W.F., Gomboc A., Kobayashi S., Margutti R., Mundell C.G. An unexpectedly small emission region size inferred from strong high-frequency diffractive scintillation in GRB 161219B. *The Astrophysical Journal*, 2019, v.870, no.2, id67, 1–12.
19. Taylor G.B., Frail D.A., Berger E., Kulkarni S.R. The angular size and proper motion of the afterglow of GRB 030329. *The Astrophysical Journal*, 2004 v.609, no.1, L1, 1–3.
20. Eichler D., Levinson A. A compact fireball model of gamma-ray bursts. *The Astrophysical Journal*, 2000, v.529, no.1, 146–150.
21. Piran T. Gamma-ray bursts and the fireball model. *Physics Reports*, 1999, v.314, no.6, 575–667.
22. Fox D.B., Mészáros P. GRB fireball physics: prompt and early emission. *New Journal of Physics*, 2006, v.8, 199–223.
23. Ciolfi R. Short gamma-ray burst central engines. *International Journal of Modern Physics D*, 2018, v.27, no.13, 1842004.
24. Levan A.J., Tanvir N.R., Starling R.L., Wiersema K., Page K.L., Perley D.A., Schulze S., Wynn G.A., Chornock R., Hjorth J., Cenko S.B. A new population of ultra-long duration gamma-ray bursts. *The Astrophysical Journal*, 2014, v.781, no.1, A13, 1–13.
25. Thompson C. A model of gamma-ray bursts. *Monthly Notices of the Royal Astronomical Society*, 1994, v.270, no.3, 480–498.
26. Mészáros P. The fireball shock model of gamma ray bursts. *AIP Conference Proceedings 2000, Jun 23*, v.522, no.1, 213–225.
27. Sarin N., Lasky P.D., Ashton G. X-ray afterglows of short gamma-ray bursts: Magnetar or Fireball? *The Astrophysical Journal*, 2019, v.872, no.1, id114, 1–6.
28. Kopač D., Mundell C.G., Japelj J., Arnold D.M., Steele I.A., Guidorzi C., Dichiara S., Kobayashi S., Gomboc A., Harrison R.M., Lamb G.P. Limits on optical polarization during the prompt phase of GRB 140430A. *The Astrophysical Journal*, 2015, v.813, no.1, id1, 1–14.
29. McDowell A., MacFadyen A. Revisiting the parameter space of binary neutron star merger event GW170817. *The Astrophysical Journal*, 2023, v.945, no.2, id135, 1–8.
30. Willingale R., Mészáros P. Gamma-ray bursts and fast transients: multi-wavelength observations and multi-messenger signals. *Space Science Reviews*, 2017, v.207, 63–86.
31. Capozziello S., Lambiase G. The emission of Gamma Ray Bursts as a test-bed for modified gravity. *Physics Letters B*, 2015, v.750, 344–347.
32. Wang Y., Jiang L.Y., Ren J. GRB 201104A: A "repetitive" short gamma-ray burst? *The Astrophysical Journal*, 2022, v.935, no.2, id179, 1–10.
33. Fraija N., Veres P. The origin of the optical flashes: The case study of GRB 080319B and GRB 130427A. *The Astrophysical Journal*, 2018, v.859, no.1, id70, 1–9.
34. Fan X., Messenger C., Heng I.S. Probing intrinsic properties of short gamma-ray bursts with gravitational waves. *Physical Review Letters*, 2017, v.119, no.18, 181102.
35. Abbott B.P., Abbott R., Abbott T.D., et al. Gravitational waves and gamma-rays from a binary neutron star merger: GW170817 and GRB 170817A. *The Astrophysical Journal Letters*, 2017, v.848, no.2, L13, 1–7.
36. Pe'Er A. Physics of Gamma-Ray Bursts Prompt Emission. *Advances in Astronomy*, 2015, no.1, 907321.
37. Piran T. The physics of gamma-ray bursts. *Reviews of Modern Physics*, 2004 v.76, no.4, 1143–1210.
38. Yu Y.W., Gao H., Wang F.Y., Zhang B.B. Gamma-Ray Bursts. *Handbook of X-ray and Gamma-ray Astrophysics*, Springer Nature Reference Book, Singapore, 2022, 34 pages.
39. Dado S., Dar A., De Rújula A. Critical Tests of Leading Gamma Ray Burst Theories. *Universe*, 2022, v.8, no.7, 350–395.
40. Yost S.A., Harrison F.A., Sari R., Frail D.A. A study of the afterglows of four gamma-ray bursts: constraining the explosion and fireball model. *The Astrophysical Journal*, 2003, v.597, no.1, 459–473.
41. Oates S.R., Page M.J., Schady P., et al. A statistical study of gamma-ray burst afterglows measured by the Swift Ultraviolet Optical Telescope. *Monthly Notices of the Royal Astronomical Society*, 2009, 395, no.1, 490–503.
42. Chandra P., Frail D.A. A radio-selected sample of gamma-ray burst afterglows. *The Astrophysical Journal*, 2012, v.746, no.2, id156, 1–28.
43. Fay S. ΛCDM periodic cosmology. *Monthly Notices of the Royal Astronomical Society*, 2020, v.494, no.2, 2183–2190.
44. Stanek K.Z., Matheson T., Garnavich P.M., et al. Spectroscopic discovery of the supernova 2003dh associated with GRB 030329. *The Astrophysical Journal*, 2003, v.591, no.1, L17, 1–3.
45. Hurley K., Sommer M., Atteia J.L., Boer M., Cline T., Cotin F., Henoux J.C., Kane S., Lowes P., Niel M. The solar X-ray/cosmic gamma-ray burst experiment aboard ULYSSES. *Astronomy and Astrophysics Supplement Series*, 1992, v.92, no.2, 401–410.
46. Bloom J.S., Berger E., Kulkarni S.R., Djorgovski S.G., Frail D.A. The redshift determination of GRB 990506 and GRB 000418 with the Echellete Spectrograph Imager on Keck. *The Astronomical Journal*, 2003, v.125, no.3, 999–1005.
47. Klose S., Stecklum B., Masetti N., et al. The very red afterglow of GRB 000418: Further evidence for dust extinction in a gamma-ray burst host galaxy. *The Astrophysical Journal*, 2000, v.545, no.1, 271–276.
48. Waxman E. The nature of GRB 980425 and the search for off-axis gamma-ray burst signatures in nearby Type Ib/c supernova emission. *The Astrophysical Journal*, 2004, v.602, no.2, 886–891.
49. Aad G., Abajyan T., Abbott B., Abdallah J., Khalek S.A., Abdelalim A.A., Aben R., Abi B., Abolins M., AbouZeid O.S., Abramowicz H. Observation of a new particle in the search for the Standard Model Higgs boson with the ATLAS detector at the LHC. *Physics Letters B*, 2012, v.716, no.1, 1–29.
50. Zhang B. A possible connection between fast radio bursts and gamma-ray bursts. *The Astrophysical Journal Letters*, 2013, v.780, no.2, L21, 1–4.
51. Jackson N. The hubble constant. *Living Reviews in Relativity*, 2015, v.18, v.1, 1–52.

52. Parker B.R. The Vindication of the Big Bang: Breakthroughs and Barriers. Springer Verlag, 2013.
53. Lian Y., Cao S., Biesiada M., Chen Y., Zhang Y., Guo W. Probing modified gravity theories with multiple measurements of high-redshift quasars. *Monthly Notices of the Royal Astronomical Society*, 2021, v.505, no.2, 2111–2123.
54. Salpeter E.E., Hoffman Jr G.L. The galaxy luminosity function and the redshift-distance controversy (a review). *Proceedings of the National Academy of Sciences*, 1986, v.83, no.10, 3056-3063.
55. Hubble E. A relation between distance and radial velocity among extragalactic nebulae. *Proceedings of the National Academy of Sciences*, 1929, v.15, no.3, 168-173.
56. Davis T. An expanding controversy. *Science*, 2019 v.365, no.6458, 1076–1077.
57. Aghanim N., Akrami Y., Ashdown M., et al. Planck 2018 results-VI. Cosmological parameters. *Astronomy & Astrophysics*, 2020, v.641, A6, 1–67.
58. Grošelj D., Sironi L., Spitkovsky A. Long-term evolution of relativistic unmagnetized collisionless shocks. *The Astrophysical Journal Letters*, 2024, v.963, no.2, L44, 1–8.
59. Kathirgamaraju A., Duran R.B., Giannios D. GRB off-axis afterglows and the emission from the accompanying supernovae. *Monthly Notices of the Royal Astronomical Society*, 2016, v.461, no.2, 1568-1575.
60. Bégué D., Burgess J.M. The anatomy of a long gamma-ray burst: a simple classification scheme for the emission mechanism(s). *The Astrophysical Journal*, 2016, v.820, no.1, id68, 1–6.
61. Sarin N., Hamburg R., Burns E., Ashton G., Lasky P.D., Lamb G.P. Low-efficiency long gamma-ray bursts: a case study with AT2020blt. *Monthly Notices of the Royal Astronomical Society*, 2022, v.512, no.1, 1391-1399.
62. Arimoto M, Asano K, Ohno M, Veres P, Axelsson M, Bissaldi E, Tachibana Y, Kawai N. High-energy non-thermal and thermal emission from GRB 141207A detected by Fermi. *The Astrophysical Journal*, 2016, v.833, no.2, id139, 1–13.
63. Zhang B.T., Murase K., Ioka K., Song D., Yuan C., Mészáros P. External inverse-Compton and proton synchrotron emission from the reverse shock as the origin of VHE gamma rays from the hyper-bright GRB 221009A. *The Astrophysical Journal Letters*, 2023, v.947, no.1, L14, 1–7.
64. Axelsson M., Borgonovo L. The width of gamma-ray burst spectra. *Monthly Notices of the Royal Astronomical Society*, 2015, v.447, no.4, 3150–3154.
65. Re'em S., Piran T. Hydrodynamic timescales and temporal structure of gamma-ray bursts. *The Astrophysical Journal*, 1995, v.455, no.2, L143–L146.
66. Rees M.J., Mészáros P. Unsteady outflow models for cosmological gamma-ray bursts. arXiv: astro-ph/9404038, 1994.
67. Fraija N., Duran R.B., Dichiara S., Beniamini P. Synchrotron self-Compton as a likely mechanism of photons beyond the synchrotron limit in GRB 190114C. *The Astrophysical Journal*, 2019, v.883, no.2, id162, 1–13.
68. Lenard P. Ueber die lichtelektrische Wirkung. *Annalen der Physik*, 1902, Bd.313, No.5, 149–198.